

Storage and Retrieval of an Image using Four-Wave Mixing in a Cold Atomic Ensemble

Jinghui Wu[†], Dongsheng Ding, Yang Liu, Zhiyuan Zhou, Baosen Shi^{††}, Xubo Zou, and Guangcan Guo
Key Laboratory of Quantum Information, Chinese Academy of Sciences, University of Science and Technology of China, Hefei, P. R. China, 230026

We realized storage and retrieval of an image of light in a cold atomic ensemble, which is obtained from a two-dimensional magneto-optical trap of Rubidium 85, using four-wave mixing. When we imprint an image on a signal laser beam, the generated idler field also carries this image information. Signal and idler are simultaneously stored in double- Λ configuration. After certain storage time, the retrieved signal and idler fields carrying this image information are observed. That means the spatial patterns of the signal and idler can be mapped into the long-lived ground state coherence of the atoms. It is worth noticing that the retrieval efficiency oscillates due to the time evolution of the ground state coherence in a uniform magnetic field. This image storage technique holds promise for application in image processing, remote sensing and quantum communication.

PACS number(s): 03.67.-a, 32.80.Qk, 42.30.-d

[†]e-mail: wjh1987@mail.ustc.edu.cn

^{††}Corresponding author: drshi@ustc.edu.cn

In the field of quantum communication, a quantum memory in which photons are stored in and then retrieved from a medium with a high efficiency is required [1]. A lot of progresses have been made in the candidate systems of quantum memories, such as cold atoms in magneto-optical trap (MOT) [2], warm atoms in vapor cells [3], Bose-Einstein condensate [4], rare-earth-doped crystals at low temperatures [5], *etc.* Usually, one-dimensional optical information is stored, such as light pulses with a uniform spatial profile (*i.e.*, no spatial information) and variation temporally only. However, the research interests have been recently extended to high-dimensional information storage (specially the spatial information), such as orbital angular momentum [6-7], transverse momentum and position [8], multiple transverse modes [9-14], *etc.* The spatial information has always been a communication medium choice because of the large amount of information they can carry. A high-dimensional state shows many interesting properties compared with a one-dimensional state.

The technique of electromagnetically induced transparency (EIT) [15,16] was successfully applied in quantum memory in a variety of systems (solid, gas). EIT can be used to make a resonant, opaque medium transparent by means of quantum interference. Meanwhile, the optical properties of the medium will be dramatically modified, *e.g.* great enhancement of nonlinear susceptibility in the spectral region of induced transparency and associated steep dispersion. This enhancement is greater in cold atoms where observable linewidths are close to natural linewidths. The steep dispersion is necessary to realize light-slowing and -storage. Because in typical storage experiments, the pulses used in them are several kilometers long in free space, which is extremely larger than the size of the storage medium (usually ranging from tens of micrometers to several centimeters). So spatially compressing the pulse in medium is primary. Then the information in the light (frequency, amplitude, phase and spatial mode, *etc.*) is mapped into long-lived atomic coherence by adiabatically switching off the control light. After sometime later, the coherences can be read out into electromagnetic field. This process can be understood in terms of a quasi-bosonic particle, a so-called dark state polariton (DSP) [17,18]. A DSP excitation consists of a photonic component and a hyperfine spin-wave (a collective matter excitation) component, in which the relative size of the light and matter components can be varied by changing the amplitude of the control light. The enhanced nonlinear susceptibility is useful in frequency mixing process, such as four-wave mixing (FWM) in cold atoms [19]. Combining the EIT and FWM, the storage of light using a FWM system have been studied [20], where the input signal and the generated idler can be simultaneously stored by switching off the pump laser. This kind of storage will improve the fidelity of storage technique for practical usage [21]. The phase

coherence between the retrieved signal and idler recently has been demonstrated [submitted]. The storage of signal and idler may have important implications in image processing, remote sensing and quantum communication, where two correlated fields need to be preserved for later use.

In this paper, we report on the storage and retrieval of an image using a FWM process based on a two-dimensional MOT [22] in an uncompensated dc magnetic field. Instead of the image itself, we mapped the Fourier transform of the image [12,14] into the atomic ensemble. This improvement can overcome the diffusion of the atoms and dramatically enhance the stability of the stored image though we have got the atoms with low enough temperature (about 100 μ K). The angle between the beams, which is tolerant in backward-wave FWM geometry, can subtract a lot of noises. This makes the storage of light in single-photon level possible. Finally, due to the Zeeman effect of the atoms in the uncompensated dc magnetic field, the retrieval efficiency shows some kind of oscillation.

The experimental setup is illustrated in Fig. 1(a). The atoms were obtained from a two-dimensional MOT [22] and the cigar-like atomic cloud is aligned in the z -axis (see, Fig. 1(a)). Three pairs of Helmholtz coils are used to generate a uniform dc magnetic field \mathbf{B} (Fig. 1(a)) in the center of the MOT (not shown). Input signal, coupling, pump and generated idler form a backward-wave FWM configuration [19]. All the beams are in the x - z plane. The coupling and the pump are collimated and coupled with each other. Signal comes out from a collimated fiber, then passes through a mask (the object), and at last is focused to the center of atomic cloud (transform plane) by lens L1 in the z -axis, which makes the optical depth of the cloud largest and coupling and pump totally overlap signal in the atomic cloud. We put the object in the front focal plane (*i.e.* object plane) of L1. The front focal plane of L2 is coincident with the back focal plane of L1 in the transform plane. Hence, the object plane, L1, transform plane, L2 and image plane (the back focal plane of L2, where we will put CCD camera or slit1) compose a $4f$ imaging system. Because of the phase-matching condition in FWM process, the divergence of idler field is the same as the convergence of signal. That means, another $4f$ imaging system consists of object, L1, transform plane, L3 and slit2 (the back focal plane of L3). The mask is just transparent in three parallel ribbons region in the y direction. The image of signal after the $4f$ system is showed in Fig. 1(b). The angle between the signal-idler axis and coupling-pump axis is 1.5 $^\circ$.

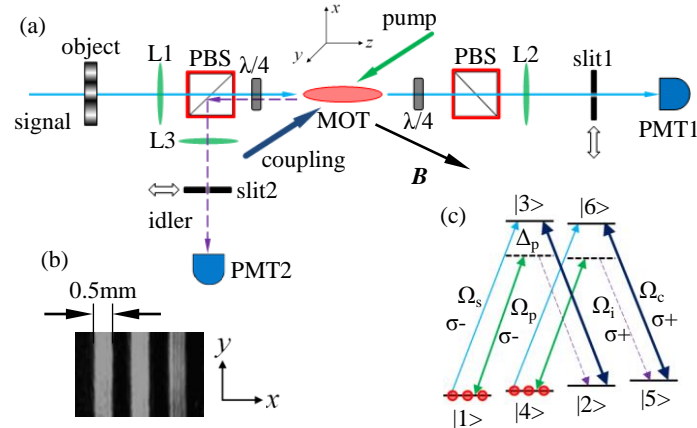


FIG. 1 (color online). (a) All the experimental laser beams come from one external-cavity diode laser (DL100, Toptica). Their frequencies are modulated by some acousto-optic modulators. The $1/e^2$ beam diameter of signal is approximately 5mm at the object plane and those of coupling and pump approximately 3.6mm and 3.2mm respectively. The peak powers of signal, coupling and pump are approximately 200pW, 200 μ W and 3.6mW respectively. Here, PBS is polarizing beam splitter; $\lambda/4$, quarter-wave plate; PMT, photomultiplier tube (Hamamatsu, H10721). The transparent windows of Slit1 and Slit2 are aligned in the y -axis. (b) The picture of signal imprinted with image. (c) The D_1 transition of ^{85}Rb creates a double- Λ configuration. Coupling is resonantly connected to transition $|2\rangle (5^2S_{1/2}, F=3, m_F=-1) \rightarrow |3\rangle (5^2P_{1/2}, F=2, m_F=-2)$, and signal is to state $|1\rangle (5^2S_{1/2}, F=3, m_F=-3)$ to state $|3\rangle$. The pump is detuned by 80MHz to the red of the optical transition connecting $|1\rangle$ and $|3\rangle$.

For the experiment, we used the Zeeman sublevels of the degenerate two-level system associated with the D_1 transition of cold ^{85}Rb atoms ($5^2S_{1/2}, F=3 \rightarrow 5^2P_{1/2}, F=2$) (Fig. 1(c)). The repetition of the experiment is 34Hz. During each experimental period, the atoms are loaded for 29.2ms, and the experimental window is 200 μ s. The cooling beams and Ioffe coils are shuttered during the experiment. But the repumper is always on to keep the atoms in the state $|5^2S_{1/2}, F=3\rangle$.

Coupling laser resonantly couples the transition $5^2S_{1/2}$, $F=3 \rightarrow 5^2P_{1/2}$, $F=2$ with $\sigma+$ polarization and signal with $\sigma-$ polarization. The strong coupling and weak signal form a generic Λ -type EIT configuration. The strong pump is σ -polarized but to the red detuning (~ 80 MHz) of D_1 transition. These three lasers compose a double- Λ FWM level system. The coupling and the pump are switched on before signal laser by $\sim 20 \mu\text{s}$ for the preparation of initial states. Hence, the atoms are appropriately pumped into the states $5^2S_{1/2}$, $F=3$, $m_F=-3$ and $m_F=-2$. Therefore, there are two independent FWM cycles (shown in Fig. 1(c)). Because of the independence of these two cycles, we will take one cycle into account below.

The time-dependent interaction Hamiltonian of the three-level Λ system showed in Fig. 1(c) is

$$H_{\text{int}} = -\frac{\hbar}{2} [(\Omega_s e^{i\Delta_s t} + \Omega_p e^{i\Delta_p t})\sigma_{31} + (\Omega_i e^{i\Delta_i t} + \Omega_c e^{i\Delta_c t})\sigma_{32} + H.c.] , \quad (1)$$

where Ω_s , Ω_p , Ω_c , Ω_i denote the Rabi frequencies of signal, pump, coupling, idler fields, Δ_m ($m=s, p, c$ and i) is the detuning of respective fields ($\Delta_s = \omega_{31} - \omega_s$, $\Delta_p = \omega_{31} - \omega_p$, $\Delta_c = \omega_{32} - \omega_c$, $\Delta_i = \omega_{32} - \omega_i$), $\sigma_{ij} = |i\rangle\langle j|$ is atomic projection operator ($i, j=1, 2, 3$), and $H.c.$ stands for Hermitian conjugate. According to energy conservation, we have $\Delta_p + \Delta_c = \Delta_s + \Delta_i$. The dynamics of laser-driven atomic system are governed by master equation for the atomic density operator:

$$\frac{d\rho}{dt} = \frac{1}{i\hbar} [H_{\text{int}}, \rho] - D . \quad (2)$$

The D is the decoherence matrix

$$D = \begin{pmatrix} -\Gamma_{31}\rho_{33} & \gamma_2\rho_{12}/2 & \gamma_{31}\rho_{13}/2 \\ \gamma_2\rho_{21}/2 & -\Gamma_{32}\rho_{33} & \gamma_{32}\rho_{23}/2 \\ \gamma_{31}\rho_{31}/2 & \gamma_{32}\rho_{32}/2 & \Gamma_3\rho_{33} \end{pmatrix} , \quad (3)$$

where Γ_{31} and Γ_{32} are the spontaneous emission rates from state $|3\rangle$ to states $|1\rangle$ and $|2\rangle$, respectively. ρ_{ij} ($i, j=1, 2, 3$) is the element of the density matrix of this system. We have also introduced energy-conserving dephasing processes with rates γ_3 and γ_2 . For convenience, we define the total spontaneous emission rate out of state $|3\rangle$ as $\Gamma_3 = \Gamma_{31} + \Gamma_{32}$. The coherence decay rates are defined as $\gamma_{31} = \Gamma_3 + \gamma_3$, $\gamma_{32} = \Gamma_3 + \gamma_3 + \gamma_2$, and $\gamma_{21} = \gamma_2$. Assuming that $\rho_{11} \approx 1$ and $\rho_{22} = \rho_{33} \approx 0$, and $\Omega_c, \Omega_p \gg \Omega_s, \Omega_i$, the steady-state solution for ρ_{12} is

$$\rho_{12} = \frac{\Omega_s \Omega_c^*}{4\Delta_1 \Delta_2 - |\Omega_c|^2} + \frac{\Omega_p \Omega_i^*}{4\Delta_2 \Delta_3 - |\Omega_p|^2} \Delta_3 / \Delta_4 , \quad (4)$$

where we have used a rotating frame to eliminate fast exponential time dependences, and $\Delta_1 = \Delta_s + i\gamma_{31}/2$, $\Delta_2 = \Delta_s - \Delta_c + i\gamma_2/2$, $\Delta_3 = \Delta_s - \Delta_c + \Delta_i + i\gamma_{31}/2$ and $\Delta_4 = -\Delta_i + i\gamma_{32}/2$ are the complex detunings respectively. In our experiment, $\Delta_s = \Delta_c = 0$ MHz, $\Delta_p = \Delta_i = 2\pi \times 80$ MHz, $\gamma_{32} \approx \gamma_{31} = 2\pi \times 3$ MHz and $\gamma_2 = 0.008\gamma_{31}$ [22].

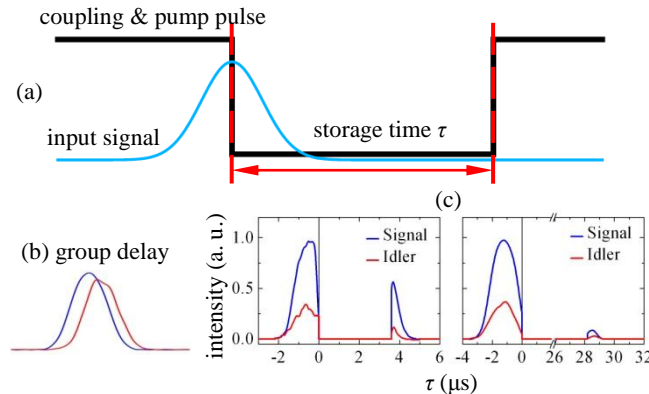


FIG. 2 (color online). (a) Representation of the synchronized timing of signal, coupling and pump. (b) Group delay of signal beams in our experiment is about $1 \mu\text{s}$. (c) Two experimental results of our FWM storage and retrieval.

The time sequence is showed in Fig. 2(a). Due to the steep dispersion of signal pulse, the group velocity will be greatly reduced (Fig. 2(b)). The delay time in our experiment is about $1 \mu\text{s}$ (pump is shuttered and coupling is constant), which can efficiently compress the signal pulse in the medium. In Fig. 2(c), we show two FWM storage and retrieval results. The full width at half maximum of the signal pulse is $1.3 \mu\text{s}$ in our experiment. In the FWM process without

storage, the images of signal and idler are shown in Fig. 3(a) and Fig. 4(a), respectively. Here, the images information is extracted by scanning the slit1 in the x -axis and slit2 in the z -axis (Fig. 1(a)). The width of the slits is 0.4mm. The same method will be used in the extraction of retrieved images. Assuming the intensities of coupling and pump are constants and they are collimated, the only spatial dependence of idler comes from the signal field amplitude. Due to the phase-matching condition $\mathbf{k}_s + \mathbf{k}_i - \mathbf{k}_c - \mathbf{k}_p = 0$, where \mathbf{k}_s , \mathbf{k}_i , \mathbf{k}_c and \mathbf{k}_p are the wave-vectors of signal, idler, coupling and pump respectively, the generated idler signal will also carry this spatial information.

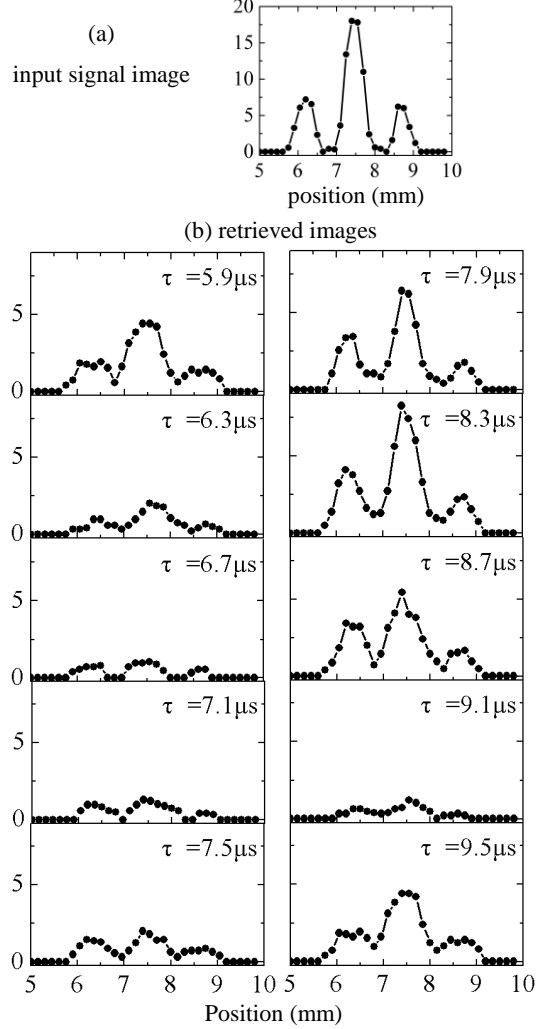


FIG. 3 (color online). (a) Input signal profile. (b) The time evolution of retrieved signal fields. We observed the oscillation of retrieved signal versus storage time τ .

Assuming the transmission of the mask is $T(x) = t^2(x)$, and the transverse profile of the light out of fiber is assumed to be Gaussian profile, $I_{s0}\exp(-x^2/d^2)$, where I_{s0} is the peak intensity of signal laser, d is the $1/e^2$ diameter of signal laser, the object's profile is $I_s(x) = T(x) \cdot I_{s0}\exp(-x^2/d^2)$, and the intensity we can get after the slit1 is indicated in Fig. 3(a). Furthermore, the vector amplitude of signal is square-root of $I_s(x)$, that is, $E_s(x) = t(x) \cdot E_{s0}\exp(-x^2/2d^2)$. At the transform plane, the amplitude of signal $E_{sf}(\xi)$ is given by the Fourier transform [14]

$$E_{sf}(\xi) = \mathcal{F}(E_s(x)) = \frac{1}{\sqrt{\lambda f}} \int_{-\infty}^{\infty} E_s(x) \exp(-i \frac{2\pi}{\lambda f} x \xi) dx, \quad (5)$$

where ξ is the coordinate of Fourier transform plane. The amplitude of idler at the transform plane is $E_{if}(\xi)$. The spatial pattern and direction of $E_{if}(\xi)$ are totally determined by the phase-matching condition. The vectorial long-lived ground state atomic coherence at the time of storage is given by [17,18]

$$\rho_2(t, \xi) = [g_s E_{sf}(\xi) + g_i E_{if}(\xi)] \exp((i\omega_{l2} - \frac{1}{2\tau})t), \quad (6)$$

where g_s and g_i are the nonlinear coupling and pump coefficients respectively, ω_{l2} is the splitting of the state $|1\rangle$ and state $|2\rangle$ in an uncompensated dc magnetic field, and τ is the coherence time of this system. Here, the diffusion of the atoms is

neglected. The magnetic field destroys the degeneracy of the ground state, and the splitting of the Zeeman sublevel cause the cosine oscillation of the retrieval efficiency, which will be discussed below. The time constant τ shows an exponential decay of the energy. As shown in Fig. 2(a), when we adiabatically turn off the coupling and pump, the signal and idler are mapped into the long-lived ground state coherence. After some time later, we turn coupling and pump on and the ground state coherence (Eq. 6) will be changed back to the electromagnetic field, *i.e.*, signal and idler. The spatial patterns of retrieved signal and idler are completely determined by the ground state coherence (coupling and pump are assumed to be constants in space) as we see from Eq. 6.

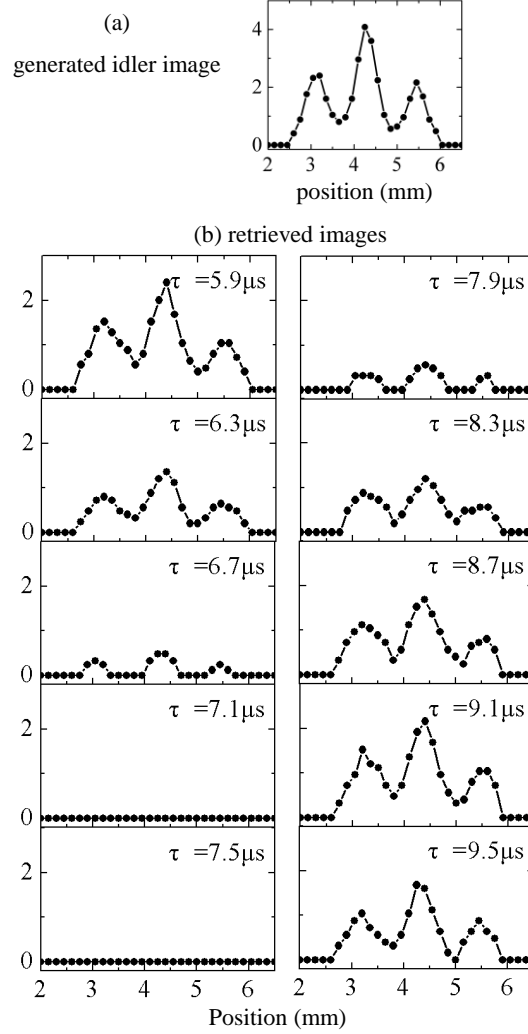


FIG. 4 (color online). (a) Generated idler profile. (b) The time evolution of retrieved idler fields. We observed the oscillation of retrieved idler versus storage time τ . The oscillating period is the same to that of signal.

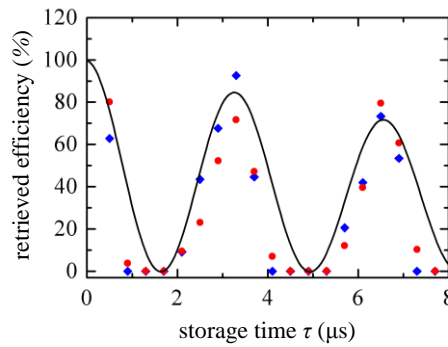


FIG. 5 (color online). The oscillation of the retrieval efficiencies of signal (blue diamonds), idler (red circles) and theoretical simulation (black line). The parameters here are period $T_{re}=3.3\mu\text{s}$, decoherence time $\tau=20\mu\text{s}$, the magnetic field $B=0.16\text{G}$ in the z -axis.

The retrieval efficiencies of signal and idler show some kind of oscillation (Fig. 3(b) and Fig. 4(b)). The phase of the

oscillation of the retrieval efficiencies is a little different, which is caused by the erratum of two measurement processes. The oscillation is caused by ground state coherence evolving temporally with frequency $\omega_{sw}=\omega_2-\omega_1$ or $\omega_5-\omega_4$. Here, ω_s ($s=1, 2, 4$ and 5) is the corresponding energy of state $|s\rangle$ in the uncompensated dc magnetic field. That means the oscillation frequency of retrieval efficiency is determined by the Zeeman effect. The retrieved efficiency is studied in Fig. 5. The period of the oscillation is $T_{re}=3.3\mu s$ and $\omega_{sw}=2\pi \Delta m \cdot g_F \cdot \mu_B B/h$, where $\Delta m=2$ in our experiment (showed in Fig. 1(c)), $g_F=1/3$ is the Lande factor for lower ground state $|5^2S_{1/2}, F=3\rangle$, μ_B is the Bohr magneton, and h is Planck constant. The period of retrieval efficiency $T_{re}=(2\pi/\omega_{sw})/2$ and the uncompensated dc magnetic field is $0.16G$ in the z -axis.

In summary, we have showed the storage and retrieval of image in a cold atomic ensemble using a FWM configuration. The backward-wave geometry and the allowed angle between signal axis and pump axis (that is tolerant in cold atoms) make storage in single-photon level possible. And because of the low temperature of atoms in MOT, the diffusion can be neglected, which enhances the fidelity of this system. Maybe it will find applications in the quantum information processing, remote sensing and image processing.

Acknowledgements

This work was supported by the National Natural Science Foundation of China (Grant Nos. 10874171, 11174271) and the National Fundamental Research Program of China (Grant No. 2011CB00200).

References

- [1] B. Julsgaard, J. Sherson, J. I. Cirac, J. Fiurasek, and E. S. Polzik, *Nature (London)*, **432**, 482 (2004).
- [2] C. Liu, Z. Dutton, C. H. Behroozi, and L. V. Hau, *Nature (London)*, **409**, 490 (2001).
- [3] D. F. Phillips, A. Fleischhauer, A. Mair, R. L. Walsworth, and M. D. Lukin, *Phys. Rev. Lett.* **86**, 783 (2001).
- [4] N. S. Ginsberg, S. R. Garner, and L. V. Hau, *Nature (London)* **445**, 623 (2007).
- [5] A. V. Turukhin, V. S. Sudarshanam, M. S. Shahriar, J. A. Musser, B. S. Ham, P. R. Hemmer, *Phys. Rev. Lett.* **88**, 023602 (2002).
- [6] L. Allen, M. W. Beijersbergen, R. J. C. Spreeuw, and J. P. Woerdman, *Phys. Rev. A* **45**, 8185 (1992).
- [7] A. Mair, A. Vaziri, G. Weihs, and A. Zeilinger, *Nature (London)*, **412**, 313 (2001).
- [8] M. O. O'Sullivan-Hale, I. A. Khan, R. W. Boyd, and J. C. Howell, *Phys. Rev. Lett.* **94**, 220501 (2005).
- [9] M. Jain, A. J. Merriam, A. Kasapi, G. Y. Yin, and S. E. Harris, *Phys. Rev. Lett.* **75**, 4385 (1995).
- [10] R. M. Camacho, C. J. Broadbent, I. A. Khan, and J. C. Howell, *Phys. Rev. Lett.* **98**, 043902 (2007).
- [11] R. Pugatch, M. Shuker, O. Firstenberg, A. Ron, and N. Davidson, *Phys. Rev. Lett.* **98**, 203601 (2007).
- [12] L. Zhao, T. Wang, Y. Xiao, and S. F. Yelin, *Phys. Rev. A* **77**, 041802(R) (2008).
- [13] M. Shuker, O. Firstenberg, R. Pugatch, A. Ben-Kish, A. Ron, and N. Davidson, *Phys. Rev. A* **76**, 023813(2007).
- [14] P. K. Vudiyasetu, R. M. Camacho, and J. C. Howell, *Phys. Rev. Lett.* **100**, 123903 (2008).
- [15] S. E. Harris, *Phys. Today* **50**, No. 7, 36 (1997).
- [16] M. Fleischhauer, A. Imamoglu, and J. P. Marangos, *Rev. Mod. Phys.* **77**, 633 (2005).
- [17] M. Fleischhauer, and M. D. Lukin, *Phys. Rev. Lett.* **84**, 5094 (2000).
- [18] M. Fleischhauer, and M. D. Lukin, *Phys. Rev. A* **65**, 022314 (2002).
- [19] D. A. Braje, V. Balic, S. Goda, G. Y. Lin, and S. E. Harris, *Phys. Rev. Lett.* **93**, 183601 (2004).
- [20] R. M. Camacho, P. K. Vudiyasetu, and J. C. Howell, *Nature Photonics*, **3**, 103 (2009).
- [21] M. Fleischhauer, *Nature Photonics*, **3**, 76 (2009).
- [22] Y. Liu, J.-H. Wu, B.-S. Shi, and G.-C. Guo, *Chin. Phys. Lett.* **29**, 024205 (2012).